

Planar Alignment of Graphene Sheets by a Rotating Magnetic Field for Full Exploitation of Graphene as a 2D Material

Feng Lin, Guang Yang, Chao Niu, Yanan Wang, Zhuan Zhu, Haokun Luo, Chong Dai, David Mayerich, Yandi Hu, Jonathan Hu, Xufeng Zhou, Zhaoping Liu, Zhiming M. Wang,* and Jiming Bao*

Planar alignment of disc-like nanomaterials is required to transfer their superior anisotropic properties from microscopic individual structures to macroscopic collective assemblies. However, such alignment by electrical or magnetic field is challenging due to their additional degrees of orientational freedom compared to that of rod-like nanostructures. Here, the realization of planar alignment of suspended graphene sheets using a rotating magnetic field produced by a pair of small NdFeB magnets and subsequent demonstration of high optical anisotropy and potential novel device applications is reported. Compared to partially aligned sheets with a static magnetic field, planar aligned graphene suspensions exhibit a near-perfect order parameter, much higher birefringence and anisotropic absorption/transmission. A unique feature of discotic nanomaterial assemblies is that the observed order parameter and optical property can vary from isotropic to partial and complete alignment depending on the experimental configuration. By immobilizing and patterning aligned graphene in a UV-curable polymer resin, we further demonstrated an all-graphene permanent display, which exhibits wide-angle, high dark-bright contrast in either transmission or reflection mode without any polarizing optics. The ability to control and pattern graphene orientation in all three dimensions opens up new exploration and broad device applications of graphene.

as graphene and transition metal dichalcogenides (TMDs).^[1] Because discotic nanostructures have more degrees of orientational freedom and a high optical anisotropy, they were anticipated to exhibit more complicated liquid crystal phases and even overcome some display problems with rod-like molecules such as its small viewing angles.^[1,2] Although the first demonstration of electrically-controlled birefringence and liquid crystal display of discotic molecules was reported in 2003, there was not much further progress since then.^[2b] A major challenge is that planar alignment of discotic molecules is difficult to achieve. Rod-like molecules can be easily aligned by an external static field, but for a discotic structure, the field line will go through the disc plane, and the disc will still have the freedom to rotate around the field line. In other words, a disc has two degrees of orientational freedom, a one-directional field is not sufficient to determine its orientation, and only partial alignment can be achieved.^[2b,3] Rotating

magnetic field was used to obtain planar alignment of mechanical reinforcing discotic materials,^[4] graphite,^[5] and reduced graphene oxide (GO) flakes,^[6] but their magnetic responses were provided by the decorated magnetic nanoparticles. Planar alignment of pure discotic particles such as Al(OH)₃, platelets and

1. Introduction

Disc-like (discotic) nanostructures encompass a wide range of materials from aromatic molecules and clay platelets to recent atomically thin two dimensional (2D) materials such

F. Lin, Dr. Y. Wang, Prof. Z. M. Wang, Prof. J. M. Bao
Institute of Fundamental and Frontier Sciences
University of Electronic Science and Technology of China
Chengdu 610054, Sichuan, China
E-mail: zhmwang@uestc.edu.cn; jbao@uh.edu

F. Lin, Dr. Y. Wang, Dr. Z. Zhu, Prof. D. Mayerich, Prof. J. M. Bao
Department of Electrical and Computer Engineering
University of Houston
Houston, TX 77204, USA

G. Yang, Prof. J. M. Bao
Department of Materials Science and Engineering
University of Houston
Houston, TX 77204, USA

 The ORCID identification number(s) for the author(s) of this article can be found under <https://doi.org/10.1002/adfm.201805255>.

C. Niu, Prof. J. Hu
Department of Electrical and Computer Engineering
Baylor University
Waco, TX 76798, USA

H. Luo
School of Optical and Electronic Information
Huazhong University of Science and Technology
Wuhan 430074, Hubei, China

Dr. C. Dai, Prof. Y. Hu
Department of Civil and Environmental Engineering
University of Houston
Houston, TX 77204, USA

Prof. X. Zhou, Prof. Z. Liu
Key Laboratory of Graphene Technologies and Applications of Zhejiang Province
Ningbo Institute of Materials Technology and Engineering
Chinese Academy of Sciences
Ningbo 315201, Zhejiang, China

DOI: 10.1002/adfm.201805255

GO were reported, but were only achieved by a rotating sample and a very strong static magnetic field (6–20 T) generated by a superconducting coil.^[7] Due to these and other reasons, many intrinsic and unique properties of aligned 2D materials have not been revealed, which hinders their device applications.^[7b]

2D nanomaterials have attracted enormous attention recently due to their excellent electronic, optical, mechanical, thermal, and various other properties. It should be noted that these properties are intrinsically anisotropic and confined to the planes of 2D materials. For large-scale macroscopic devices that require thousands or millions of individual 2D nanostructures, it is extremely important to control the orientation of individual units and align their planes parallel with each other. Only with this planar alignment of 2D nanomaterials can their unique microscopic properties be transferred to large-scale devices. As such, many techniques have been developed, including those based on mechanical shear force or the Langmuir–Blodgett surface method,^[8] and excellent performances of aligned graphene have been demonstrated, such as electromagnetic interference shielding,^[9] optical display,^[8a,10] ultrahigh thermal conductivity,^[11] and transparent conducting thin films.^[8b,12] However, these mechanical or chemical force-based techniques suffer from many serious shortcomings. For instance, orientations cannot be arbitrarily controlled, especially with respect to their supporting substrate,^[12,13] making it difficult to achieve a large-scale uniform alignment, and the alignment procedure can hardly be compatible with other fabrication processes such as patterning. A non-contact field-controlled planar alignment is highly desired.

In this work, we demonstrate planar alignment of suspended graphene sheets using a weak rotating magnetic field produced by a pair of small commercial magnets. We achieve extraordinary anisotropic optical properties of aligned graphene such as strong birefringence and polarization-dependent transmission/absorption. Our experiments have also revealed a significant difference between aligned one dimensional (1D) and 2D nanomaterials:

the measured order parameter and optical anisotropy of 2D nanomaterial assembly are strongly dependent on the experimental configuration and can be controlled by two degrees of orientational freedom.^[3f] To demonstrate the flexibility of magnetic alignment and unique optical properties of aligned graphene, we created the first dual-mode all-graphene permanent display using UV-assisted polymer immobilization and patterning of graphene sheets. This display is omnidirectional without additional polarizing optics, and it exemplifies all the advantages of 2D materials that cannot be realized by rod-like molecules or nanomaterials.

2. Results and Discussion

Graphene sheets were fabricated with electrochemical exfoliation of highly oriented pyrolytic graphite (HOPG) in a salt solution and dispersed in *N*-methyl-2-pyrrolidone (NMP).^[13] Figure 1a shows our magnetic technique to align graphene sheets parallel to a plane. A glass cell/cuvette filled with graphene suspension is placed between two 1 in. NdFeB magnet cubes, which are mounted on a motor to produce a horizontal rotating magnetic field at a speed of 5–15 revolutions per second. Compared with the previous technique using a single rotating magnet, our design can produce a more uniform field with an adjustable magnetic field strength over a large distance.^[4–6] Because of their strong diamagnetic properties,^[3f,g] the graphene sheets will be aligned in the *x*–*y* plane swept by the rotating magnetic field.^[3f,14]

The effect of a rotating magnetic field on the graphene alignment can be conveniently observed with birefringence images as shown in Figure 1b–d: planar aligned graphene exhibits a much stronger birefringence compared to partially aligned graphene by a static magnetic field. A uniform birefringence image indicates a uniform alignment over the whole cuvette. Figure 1e confirms that the birefringent transmission is four times stronger with the rotating field than that with the static

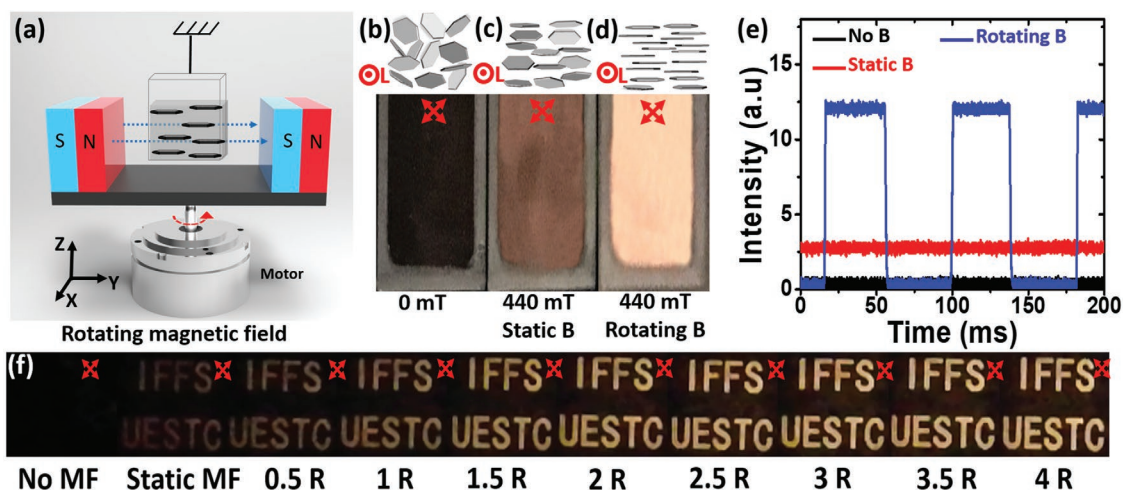


Figure 1. Planar alignment of graphene sheets and their strong birefringence. a) Schematic of experimental setup to generate a rotating magnetic field in the *x*–*y* plane. b–d) Schematics of graphene orientations and snapshots of white light birefringence/transmission images of graphene suspension in a 1 cm cuvette between two cross-polarizers (polarization indicated by red arrows) under (b) zero magnetic field, (c) static magnetic field in the *y*-direction, and (d) rotating magnetic field in the *x*–*y* plane. The incident white light is in the *x*-direction, indicated by “L.” e) Transmission of 632.8 nm laser through the same graphene suspension as in (b–d). The transmission was measured with a photodiode and an oscilloscope, the zero transmission with rotating magnetic field is due to the blocking of laser by the rotating magnets. f) Evolution of birefringence image of “IFFS UESTC” as the magnetic field begins to rotate. R: revolution; MF: magnetic field.

field. The alignment difference between a static and rotating magnetic field can be clearly seen from the schematics of graphene orientations in **Figure 2c,d**. Under a static field in y -direction, each graphene becomes aligned in the y -direction due to the interaction between magnetic field and its induced current in graphene, but each is still free to rotate around the y -direction.^[3c,d,f,g] A naive way to align the graphene to the x -direction at the same time is to apply another magnetic field in the x -direction. Unfortunately, this method will not work because magnetic field is a vector; a combination of two fields in the x and y directions will simply result in a new field at 45° to x and y , assuming both fields have the same magnitude. One way to get around it is to use a rotating field: at each moment, there is only one field, and the alignments in x and y directions, strictly speaking every direction in the x - y plane, are performed alternatively and repeatedly by the rotating field.

To find out the time required for planar alignment, we monitored the birefringence transmission image once the magnets began to rotate. **Figure 1f** shows that a stable planar alignment can be achieved only after four revolutions of magnetic field in 3-4 s. Another unique property of 2D graphene is that the degree

of alignment is dependent on the rotation speed. **Figure S1** in the Supporting Information shows that the birefringent transmission decreases rapidly if the rotation speed falls below 5 revolutions per second. More research is needed to understand the dynamics of graphene planar alignment; we believe this time scale is related to the relaxation of graphene orientation. For a very slow rotational speed, the time between two consecutive alignments after half a rotation, i.e., in the x -direction, becomes much longer than the orientation relaxation time; as a result, the previous alignment becomes either lost or cannot be further improved, leading to a low overall alignment order.

Such strong optical birefringence must come from a high alignment order of graphene sheets, which can be verified by a strong polarization-dependent optical transmittance as shown in **Figure 2a**. Conversely, we can calculate the alignment order parameter based on such anisotropic optical transmission $S = \frac{1-\Delta}{1+\Delta/2}$, where $\Delta = k_{\perp}/k_{\parallel}$, and k is the extinction coefficient.^[15] **Figure 2c** shows that the order parameter of graphene in a rotating magnetic field increases almost linearly at a low rotating magnetic field, but starts to saturate when it reaches 0.8 at 440 mT. As a comparison, results perpendicular to a static magnetic

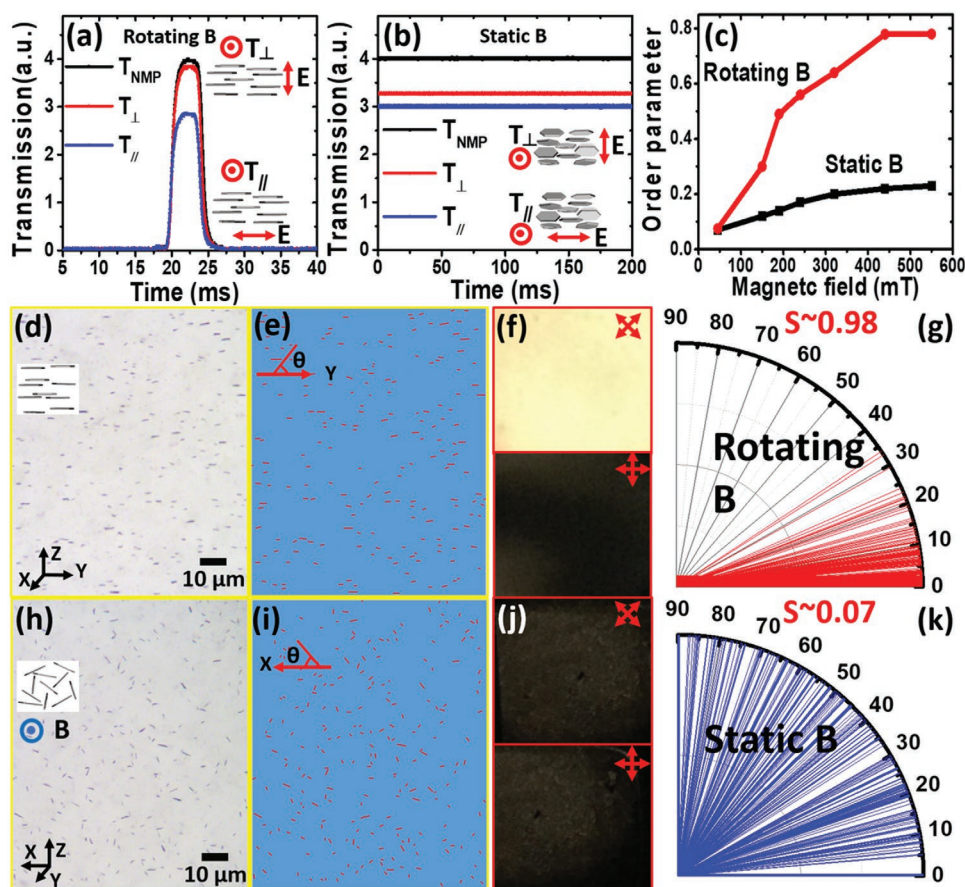


Figure 2. Order parameter of aligned graphene measured with anisotropic optical transmission and microscope images under different magnetic field strengths and experimental configurations. a,b) Polarization-dependent optical transmission of 632.8 nm laser through suspended graphene sheets aligned by (a) a rotating magnetic field and (b) a static magnetic field as in **Figure 1e** at 440 mT. T_{NMP} is the reference transmission of NMP without graphene. c) Calculated order parameters as a function of magnetic field based on the anisotropic transmission in (a) and (b). d,e,h,i) Microscopic raw and processed images of graphene aligned with the same (d,e) rotating and (h,i) static magnetic field as in (a) and (b) except that graphene sheets are immobilized in a UV-curable resin. The θ in (e,i) is the angle between graphene sheet and x - y plane. f,j) White light birefringence images of graphene polymer films in (d) and (h). g,k) Polar histograms of angle θ in (e,i) and corresponding alignment order parameters.

field are included in Figure 2b,c: the transmission is weakly dependent on the polarization and the order parameter saturates at 0.2, indicating a very low degree of alignment perpendicular to the magnetic field. As discussed above, graphene sheets are only partially aligned along the magnetic field direction and they can still randomly rotate around the magnetic field.^[16]

Note that the polarization-dependent optical absorption is mainly due to the shape anisotropy of graphene. The electrons have a high mobility in the graphene plane, but cannot easily move in the direction perpendicular to the plane. Under an in-plane electrical field, a large polarization is induced, resulting in strong optical absorption and weak optical transmission. Nevertheless, the order parameter of 0.8 does not reflect the actual alignment of graphene sheets. In fact, order parameter obtained from the above anisotropic optical absorption is not well applicable to our multilayer graphene (average thickness is 2 nm) because a perfect alignment (order parameter of 1) requires a zero k_{\perp} , which can only be achieved by single layer graphene.^[15a,17] To better characterize the alignment, we took microscopic images of graphene sheets and measured their actual orientations with respect to the applied magnetic field. Figure 2d,e,g reveals that graphene sheets are well oriented in the rotating field of x - y plane with a small angle θ distribution. A high order parameter of 0.98 is obtained based on $S = \langle 2\cos^2\theta - 1 \rangle$,^[17] in agreement with the simulation in Figure S2 in the Supporting Information. In contrast, Figure 2h,i,k shows that graphene sheets are randomly oriented in the direction perpendicular to the static magnetic field, giving us a near-zero order parameter. These extreme order parameters can be quickly confirmed by

birefringence images in Figure 2f,j: graphene sheets aligned by a static magnetic field is optically isotropic in the direction of the field. Note that this zero order parameter does not contradict the order parameter obtained by polarized absorption in Figure 2b,c; the difference comes from different observations or experimental configurations, which is unique to 2D nanomaterials.

A better way to distinguish partially and planar aligned graphene sheets in Figure 2a–c is to simply send a laser beam through the graphene suspension and observe the transmitted or diffracted beam pattern. Figure 3a shows the schematic of the laser diffraction setup. Figure 3c,e,i shows diffracted laser beam after going through NMP; NMP with graphene sheets aligned by the static and rotating magnetic fields. Figure 3d,h shows schematics of graphene orientations. The difference is obvious: an almost uniformly enlarged laser spot versus vertical diffraction pattern. The former indicates light scattering by randomly oriented graphene sheets, while the latter confirms planar alignment of graphene sheets in the horizontal direction.

Our uniform large-volume magnetic alignment is compatible with additional control or manipulation of graphene sheets. By dispersing graphene in a mixed solution of NMP and UV-curable adhesive, we can use UV light (365 nm) to polymerize the solution and make the alignment permanent. Figure 3b shows pictures of a pure polymer film and two graphene/polymer composite films. Figure 3f,g,j shows similar diffraction patterns through the polymer and graphene/polymer composite films, indicating a successful immobilization of graphene orientation. A sharper diffraction in Figure 3j than in Figure 3i is due to the reduced Brownian

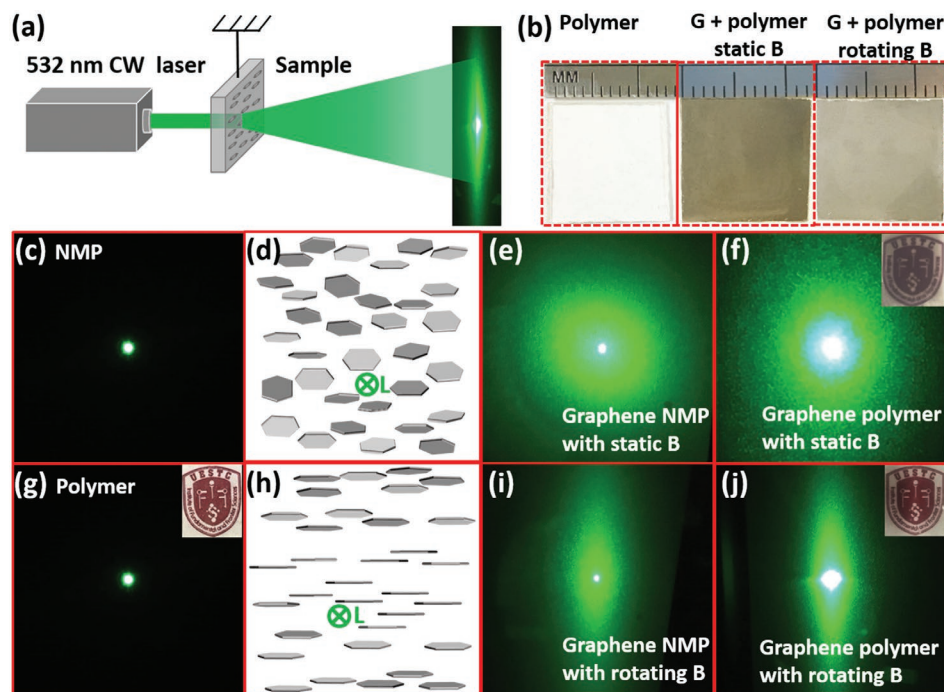


Figure 3. Diffraction and transmission through aligned graphene sheets. a) Schematic of far-field laser diffraction. b) Images of polymerized thin films of UV-curable optical adhesive (left) without graphene, (middle) partially aligned graphene, and (right) planar aligned graphene with schematic orientations shown in (d) and (h). c–f) Comparison of far-field diffraction patterns of the laser beam through (c) NMP solution without graphene, (e,f) graphene sheets in NMP and polymer aligned by a static field. (d) is the schematic of graphene orientations with respect to the incident laser beam. g–j) Same as (c–f), but graphene is aligned by a rotating field. Insets in (f), (g), and (j) are images of polymer w/o graphene thin films on an “IFFS” logo.

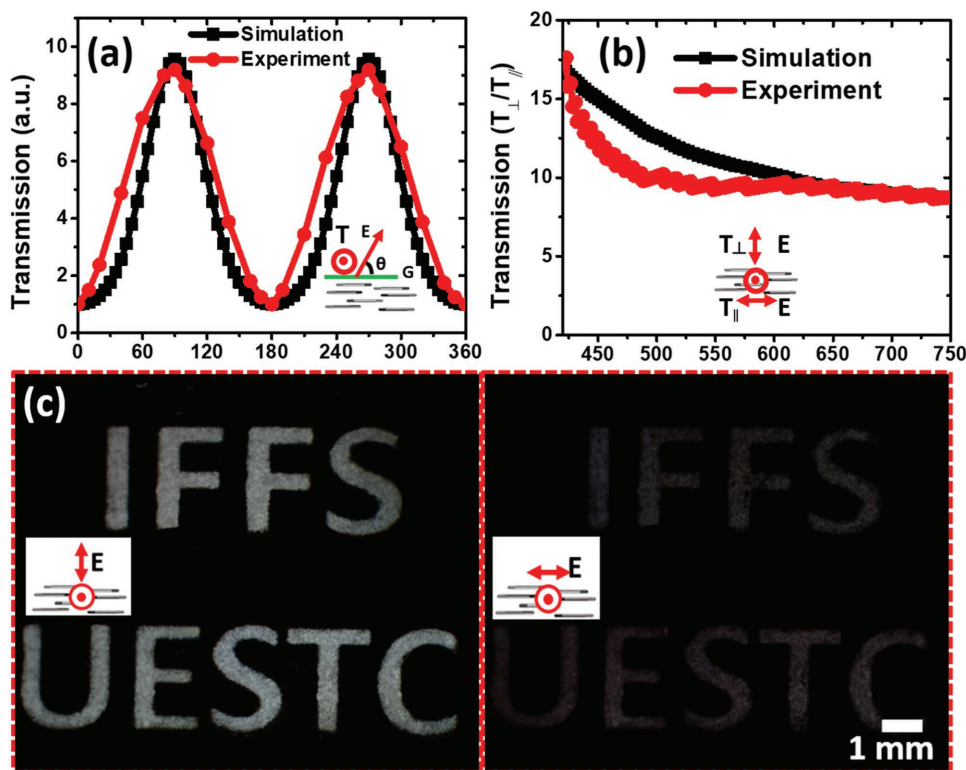


Figure 4. Polarization-dependent optical transmission of planar aligned graphene sheets immobilized in a polymer resin. a) Measured and calculated optical transmissions as a function of angle between graphene plane and polarization. The minimum transmission of light polarized parallel to the graphene plane is chosen as a reference. b) Measured and simulated extinction ratio in the visible spectrum. c) The same graphene polarizer used as a polarization switchable transmission optical display using a photomask. Red arrows indicate light polarization direction.

motion and disturbance in polymer films.^[18] The insets show the transparency of these films for incoherent white light. Due to large lateral size (1.5 μm on average), graphene sheets strongly scatter light when randomly oriented, but once they are aligned, light scattering and diffusion are greatly reduced and transparency is increased.^[19]

The ability to immobilize graphene orientation enables us to demonstrate several optical devices. The most obvious device is the optical polarizer based on polarization-dependent transmission in Figure 2. In fact, the graphene/polymer film in the right of Figure 3b is already such a device where graphene sheets are aligned perpendicular to the film plane. Figure 4a shows the ratio of transmission as a function of the angle between light polarization and the graphene plane. As expected for a polarizer, the transmission oscillates between two polarizations. It is worth noting that the high extinction ratio of 10:1 of this graphene polarizer is either much higher than that of aligned organic nanocrystal polarizer or comparable to that of aligned carbon nanotubes (CNT) film.^[20] Figure 4b shows that the high extinction ratio is maintained over the whole visible spectrum and is broader than CNT-based polarizer.^[20b] All these excellent anisotropic properties originate from underlying graphene sheets, and the results are well reproduced by simulations shown in Figure 4a,b.^[21] The small discrepancy is believed to come from the broad size distribution of graphene sheets in the experiment. By the way, graphene sheets are completely aligned in the simulation. A good agreement between experiment and

simulation in the optical transmission anisotropy indicates a perfect alignment in the experiment. As a side application, Figure 4c shows a simple polarization-controlled transmission display using a photomask and an ordinary polarizer.

The unique advantage of our magnetic alignment, i.e., a small magnet footprint but with uniform alignment over a large volume, further allows us to create arbitrary patterns of aligned graphene for various applications. Figure 5a shows an example of two-step patterning of graphene sheets aligned in two directions using UV-assisted orientation immobilization. Multiple steps are needed to pattern graphene sheets in multiple directions, with each step immobilizing one orientation. Figure 5b,c,e,f shows an all-graphene display of a baby panda in either transmission or reflection mode with a complementary contrast. Here the diffuse reflection display was implemented by placing the graphene panda film on a dark background under white light. The bright (dark) area in the reflection mode has graphene sheets aligned parallel (perpendicular) to the film surface. Such bright-dark contrast is a result of unique orientation-dependent optical transmission and reflection of graphene, which again can be well understood through simulations in Figure 5d,g.^[3f,22] Like many other display techniques, the resolution of our graphene display is limited by photolithography, graphene size, and the film thickness, which is 1 mm for the panda film. Figure S4 in the Supporting Information shows microscopic optical images of bright/dark transition regions of the display: a

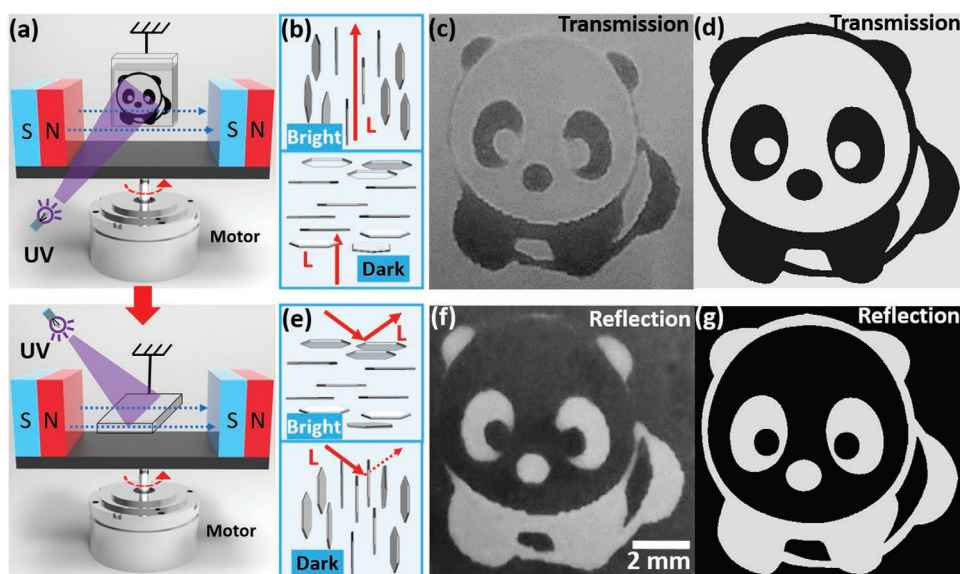


Figure 5. Patterned graphene thin film display. a) Two steps to pattern graphene aligned in normal and parallel to the graphene/polymer film. b–d) Transmission and simulated transmission images of patterned graphene panda. (b) Two graphene orientations in the bright and dark regions of the panda relative to the incident light in transmission. e–g) Same as (b–d), but in the reflection mode.

sharp transition can be observed in both reflection and transmission mode. A resolution on the micrometer scale should be achieved in principle by using smaller size graphene and thinner display films.

Although transmissive/reflective display with graphene or GO has been realized before, the current display using planar aligned graphene offers higher contrast and wider viewing angle. Such advantage comes from well dispersed while parallel graphene sheets, and can be easily understood via the schematics in Figure 5b,e. In previous GO display, only part of GO sheets in contact with the stick become aligned;^[8a] while with a static magnetic field, randomly or partially oriented graphene sheets have much less contrast between reflection versus transmission.^[3f] Maximum reflection and transmission can only be achieved with planar aligned graphene sheets, leading to the highest bright/dark contrast.^[3a,6,8a] Figure S5 in the Supporting Information shows that the contrast is almost maintained over nearly 180° of viewing. Such large viewing angle is due to the unique and very distinct surface textures: a flat smooth surface when graphene is aligned parallel to the display surface versus a rough spiky surface when aligned perpendicular to the surface, and the optical properties of both types of surfaces are insensitive to the direction of incident light. Clearly, these properties and applications are unique to discotic materials and cannot be realized by 1D nanostructures.

3. Conclusions

In summary, we have demonstrated a low cost, fast, and simple magnetic method to produce planar aligned graphene sheets with a high order parameter over a large volume. We also revealed extraordinary anisotropic optical properties and demonstrated several unique optical devices of aligned graphene.

Compared to 1D nanostructures, discotic materials exhibit a measurement configuration-dependent order parameter, which can be further controlled by either a static or rotating magnetic field. The benefits of aligned graphene are exemplified in an all-graphene display, and these benefits are applicable to other properties of graphene. As a non-contact method, magnetic alignment can be integrated with many other patterning techniques to create three dimensional complex structures of aligned graphene domains with different novel properties. This simple planar alignment of graphene will accelerate applications of graphene in many other fields.^[5–7,9b,12,23] As the strongest diamagnetic nanomaterial, graphene sheets can also be used as a vehicle to control and align other low dimensional nanomaterials or composites.

4. Experimental Section

Preparation of Graphene NMP Suspension and Graphene Polymer Resin: Graphene was obtained by electrochemical exfoliation of HOPG in K_2SO_4 salt solution,^[13] and dispersed in NMP and ultra-sonicated for 2 h. Average size of the multi-layer graphene was around 1.5 μm with 2.4 nm thickness. Graphene polymer resin was fabricated by mixing multi-layer graphene NMP suspension (0.05 wt%), polyethylene glycol diacrylate (PEGDA, Mn: 700) and UV-curable adhesive (volume ratio: 2:1:1). PEGDA was purchased from Sigma-Aldrich and UV-cured optical adhesives (NOA65) was purchased from Thorlabs.

Measurement of Birefringence: Field-induced birefringence was measured with a cuvette (thickness: 1 mm) filled with multi-layer graphene NMP dispersion (0.05 wt%) and placed between the two magnets. Two crossed polarizers were placed in the front and back of the cuvette with 45° relative to the magnetic field. For birefringence images in Figure 1b–d,f, a tungsten lamp was used as a light source and a mobile phone camera was used to capture the video. For relative transmission in Figure 1e, a 632.8 nm laser was used as a light source, and the transmitted laser was detected by a photodiode and a scope.

Supporting Information

Supporting Information is available from the Wiley Online Library or from the author.

Acknowledgements

F.L. was supported by Academic Special Fund from University of Electronic Science and Technology of China and China Scholarship Council. J.M.B. acknowledges support from Welch Foundation (E-1728) and National Science Foundation (EEC-1530753). J.H. acknowledges support from National Science Foundation (ECCS-1809622).

Conflict of Interest

The authors declare no conflict of interest.

Keywords

2D materials, graphene alignment, graphene display, planar alignment, rotating magnetic field

Received: July 30, 2018
Revised: September 3, 2018
Published online:

-
- [1] a) T. Wohrle, I. Wurzbach, J. Kirres, A. Kostidou, N. Kapernaum, J. Litterscheidt, J. C. Haenle, P. Staffeld, A. Baro, F. Giesselmann, S. Laschat, *Chem. Rev.* **2016**, *116*, 1139; b) M. Kumar, A. Gowda, S. Kumar, *Part. Part. Syst. Charact.* **2017**, *34*, 1700003; c) M. Mathews, Q. Li, *Self-Organized Organic Semiconductors: From Materials to Device Applications*, John Wiley & Sons, Inc., Hoboken, New Jersey **2011**, pp. 83–129, Ch. 4.
- [2] a) B. R. Kaafarani, *Chem. Mater.* **2011**, *23*, 378; b) G. G. Nair, D. S. S. Rao, S. K. Prasad, S. Chandrasekhar, S. Kumar, *Mol. Cryst. Liq. Cryst.* **2003**, *397*, 245.
- [3] a) T. Z. Shen, S. H. Hong, J. K. Song, *Nat. Mater.* **2014**, *13*, 394; b) D. Rossi, J. H. Han, W. Jung, J. Cheon, D. H. Son, *ACS Nano* **2015**, *9*, 8037; c) I. O. Shklyarevskiy, P. Jonkheijm, N. Stutzmann, D. Wasserberg, H. J. Wondergem, P. C. Christianen, A. P. Schenning, D. M. de Leeuw, Z. Tomovic, J. Wu, K. Mullen, J. C. Maan, *J. Am. Chem. Soc.* **2005**, *127*, 16233; d) L. Wu, M. Ohtani, M. Takata, A. Saeki, S. Seki, Y. Ishida, T. Aida, *ACS Nano* **2014**, *8*, 4640; e) H.-S. Kim, S.-M. Choi, J.-H. Lee, P. Busch, S. J. Koza, E. A. Verploegen, B. D. Pate, *Adv. Mater.* **2008**, *20*, 1105; f) F. Lin, Z. Zhu, X. Zhou, W. Qiu, C. Niu, J. Hu, K. Dahal, Y. Wang, Z. Zhao, Z. Ren, D. Litvinov, Z. Liu, Z. M. Wang, J. Bao, *Adv. Mater.* **2017**, *29*, 1604453; g) C. Niu, F. Lin, Z. M. Wang, J. Bao, J. Hu, *J. Appl. Phys.* **2018**, *123*, 044302.
- [4] R. M. Erb, R. Libanori, N. Rothfuchs, A. R. Studart, *Science* **2012**, *335*, 199.
- [5] J. Billaud, F. Bouville, T. Magrini, C. Villevieille, A. R. Studart, *Nat. Energy* **2016**, *1*, 16097.
- [6] H. Le Ferrand, S. Bolisetty, A. F. Demirors, R. Libanori, A. R. Studart, R. Mezzenga, *Nat. Commun.* **2016**, *7*, 12078.
- [7] a) X. Lu, X. Feng, J. R. Werber, C. Chu, I. Zucker, J. H. Kim, C. O. Osuji, M. Elimelech, *Proc. Natl. Acad. Sci. U. S. A.* **2017**, *114*, E9793; b) D. van der Beek, A. V. Petukhov, P. Davidson, J. Ferre, J. P. Jamet, H. H. Wensink, G. J. Vroege, W. Bras, H. N. Lekkerkerker, *Phys. Rev. E* **2006**, *73*, 041402.
- [8] a) L. He, J. Ye, M. Shuai, Z. Zhu, X. Zhou, Y. Wang, Y. Li, Z. Su, H. Zhang, Y. Chen, Z. Liu, Z. Cheng, J. Bao, *Nanoscale* **2015**, *7*, 1616; b) L. J. Cote, F. Kim, J. Huang, *J. Am. Chem. Soc.* **2009**, *131*, 1043.
- [9] a) F. Shahzad, M. Alhabeab, C. B. Hatter, B. Anasori, S. Man Hong, C. M. Koo, Y. Gogotsi, *Science* **2016**, *353*, 1137; b) W. L. Song, M. S. Cao, M. M. Lu, J. Yang, H. F. Ju, Z. L. Hou, J. Liu, J. Yuan, L. Z. Fan, *Nanotechnology* **2013**, *24*, 115708; c) A. Akbari, P. Sheath, S. T. Martin, D. B. Shinde, M. Shaibani, P. C. Banerjee, R. Tkacz, D. Bhattacharyya, M. Majumder, *Nat. Commun.* **2016**, *7*, 10891.
- [10] F. Lin, X. Tong, Y. Wang, J. Bao, Z. M. Wang, *Nanoscale Res. Lett.* **2015**, *10*, 435.
- [11] Q. Li, Y. Guo, W. Li, S. Qiu, C. Zhu, X. Wei, M. Chen, C. Liu, S. Liao, Y. Gong, A. K. Mishra, L. Liu, *Chem. Mater.* **2014**, *26*, 4459.
- [12] Q. Zheng, W. H. Ip, X. Lin, N. Yousefi, K. K. Yeung, Z. Li, J. K. Kim, *ACS Nano* **2011**, *5*, 6039.
- [13] K. Parvez, Z. S. Wu, R. Li, X. Liu, R. Graf, X. Feng, K. Mullen, *J. Am. Chem. Soc.* **2014**, *136*, 6083.
- [14] Y. Ominato, M. Koshino, *Phys. Rev. B* **2013**, *87*, 115433.
- [15] a) B. Dan, N. Behabtu, A. Martinez, J. S. Evans, D. V. Kosynkin, J. M. Tour, M. Pasquali, I. I. Smalyukh, *Soft Matter* **2011**, *7*, 11154; b) Y. A. Nastishin, H. Liu, T. Schneider, V. Nazarenko, R. Vasyuta, S. V. Shiyankovskii, O. D. Lavrentovich, *Phys. Rev. E* **2005**, *72*, 041711.
- [16] M. Liu, Y. Ishida, Y. Ebina, T. Sasaki, T. Hikima, M. Takata, T. Aida, *Nature* **2015**, *517*, 68.
- [17] C. Zamora-Ledezma, C. Blanc, M. Maugey, C. Zakri, P. Poulin, E. Anglaret, *Nano Lett.* **2008**, *8*, 4103.
- [18] Y. Wang, Y. Tang, P. Cheng, X. Zhou, Z. Zhu, Z. Liu, D. Liu, Z. Wang, J. Bao, *Nanoscale* **2017**, *9*, 3547.
- [19] a) H. Wilson, W. Eck, *Sol. Energy Mater. Sol. Cells* **1993**, *31*, 197; b) C. M. Lampert, *Sol. Energy Mater. Sol. Cells* **2003**, *76*, 489; c) J. L. West, G. Zhang, A. Glushchenko, Y. Reznikov, *Appl. Phys. Lett.* **2005**, *86*, 031111.
- [20] a) Y. Kaneko, S. Shimada, T. Fukuda, T. Kimura, H. Yokoi, H. Matsuda, T. Onodera, H. Kasai, S. Okada, H. Oikawa, H. Nakanishi, *Adv. Mater.* **2005**, *17*, 160; b) X. He, W. Gao, L. Xie, B. Li, Q. Zhang, S. Lei, J. M. Robinson, E. H. Haroz, S. K. Doorn, W. Wang, R. Vajtai, P. M. Ajayan, W. W. Adams, R. H. Hauge, J. Kono, *Nat. Nanotechnol.* **2016**, *11*, 633.
- [21] F. J. Nelson, V. K. Kamineni, T. Zhang, E. S. Comfort, J. U. Lee, A. C. Diebold, *Appl. Phys. Lett.* **2010**, *97*, 253110.
- [22] M. Wang, L. He, S. Zorba, Y. Yin, *Nano Lett.* **2014**, *14*, 3966.
- [23] a) Y. Yoon, K. Lee, S. Kwon, S. Seo, H. Yoo, S. Kim, Y. Shin, Y. Park, D. Kim, J. Y. Choi, H. Lee, *ACS Nano* **2014**, *8*, 4580; b) P. Zhang, J. Li, L. Lv, Y. Zhao, L. Qu, *ACS Nano* **2017**, *11*, 5087.